

Impact behaviour of microwave-assisted compression moulded HDPE/kenaf and HDPE/MWCNT composites

A thesis

Submitted by

Nayan Pundhir

(S16009)

Partial fulfilment of the requirement for the degree of

MASTER OF SCIENCE (BY RESEARCH)

Under the guidance of

Dr. Sunny Zafar and Dr. Himanshu Pathak

(School of Engineering)



INDIAN INSTITUTE OF TECHNOLOGY MANDI

KAMAND, MANDI-175005

HIMACHAL PRADESH, INDIA

July, 2020

Acknowledgement

It is an honour for me to thank all the people who have made this thesis possible. First and foremost I offer my sincere gratitude to my thesis supervisors **Dr. Sunny Zafar** and **Dr. Himanshu Pathak**. In every sense, this work would not have been possible without their constant encouragement, valuable guidance, support and patience during the research.

I would like to thank all the APC members, lab staff, members of the School of Engineering for their support. I am very much thankful to the **Ministry of Human Resource Development, Government of India** for providing financial support for the thesis work.

I would also like to thank my lab members and friends for their support, suggestion, and making the journey enjoyable. My deepest gratitude goes to my parents for their unparallel contribution and blessings.



Nayan Pundhir

Enrollment No. S16009

Candidate's declaration

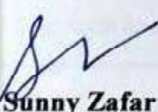
This is to certify that the thesis entitled "**Impact behaviour of microwave-assisted compression moulded HDPE/kenaf and HDPE/MWCNT composites**", submitted by me to the Indian Institute of Technology Mandi for the award of the Degree of Master of Science (by Research) is a bonafide record of research work carried out by me under the supervision of Dr. Sunny Zafar and Dr. Himanshu Pathak. The content of this thesis, in full or in parts, have not been submitted to any other institute or university for the award of any degree or diploma.



Nayan Pundhir
Enrollment No. S16009

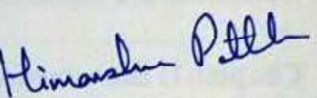
Declaration by the Thesis Supervisor

This is to certify that the thesis entitled "**Impact behaviour of microwave-assisted compression moulded HDPE/kenaf and HDPE/MWCNT composites**", submitted by **Nayan Pundhir** to the Indian Institute of Technology Mandi for the award of the Degree of Master of Science (by Research) is a bonafide record of research work carried out by him under our supervision. The content of this thesis, in full or in parts, have not been submitted to any other institute or university for the award of any degree or diploma.



Dr. Sunny Zafar

**School of Engineering
Indian Institute of Technology Mandi**



Dr. Himanshu Pathak

**School of Engineering
Indian Institute of Technology Mandi**

Table of Contents

Acknowledgement	i
Candidate's declaration.....	ii
Declaration by the Thesis Supervisor	Error! Bookmark not defined.
List of figures.....	vii
List of tables.....	xii
Abstract.....	xiii
Nomenclature	xiv
Chapter 1: Introduction	1
1.1. Classification of Impact loading	1
1.2. Composite materials.....	3
1.3. Microwave processing of materials.....	6
1.4. Application of polymer composites for crashworthiness	7
1.5. Thesis overview.....	10
1.6. Summary	11
Chapter 2: Literature Review.....	12
2.1. Literature study	12
2.2. Motivation and Research gap.....	25
2.3. Objectives and scope of the work	27
2.3.1. Objectives of the present work	27

2.3.2. Scope of the present work	27
2.4. Plan of the present work.....	28
2.5. Summary	30
Chapter 3: Fabrication and characterization.....	31
3.1. Experimental Procedure	31
3.1.1. Materials	32
3.1.2. Fibre treatment.....	35
3.1.3. Fabrication of composites.....	36
3.1.4. Characterization of the composites.....	41
3.2. Results and discussion.....	44
3.2.1. Tensile test.....	44
3.2.2. Strain-rate dependent tensile test.....	47
3.2.3. Multi-step stress relaxation test	50
3.2.4. Flexural test	51
3.2.5. Izod impact test.....	53
3.3. Summary	56
Chapter 4: Crashworthiness Analysis of HDPE Composites for the Automobile Applications	57
4.1. Governing equations	58
4.2. Problem formulation	59
4.3. Results and discussion.....	62
4.3.1. Validation and convergence study of the numerical model	62

Case I: Impact of body panel on a rigid wall.....	64
4.3.2. Geometry and modelling	65
4.3.3. Boundary conditions.....	68
4.3.4. Material properties.....	68
4.3.5. Full frontal impact	70
4.3.6. Offset frontal impact.....	77
4.3.7. Oblique frontal impact.....	83
Case II: Impact of body panel on a rigid pole	96
4.3.8. Effect of material on the von Mises stress.....	98
4.3.9. Effect of material on the directional deformation	100
4.4. Summary	110
Chapter 5: Conclusions and Scope for Future Work	111
5.1. Conclusions	111
5.1.1. Fabrication and testing of composites	112
5.1.2. Numerical study.....	113
5.2. Limitations of the present work	114
5.3. Scope for future work.....	114
References.....	115
Publications	127

List of Figures

Figure 1.1: Classification of impact.....	2
Figure 1.2: Advantages of polymer composites.	3
Figure 1.3: Advantages of natural fibres over synthetic fibres.	5
Figure 1.4: Development of microwave processing of materials and their application areas (Mishra and Sharma, 2016).....	7
Figure 1.5: Advances in body panel material (data from Gopalkrishna <i>et al.</i> , 2014).....	9
Figure 2.1: Schematic representation of the dielectric behaviour of polar polymers at different frequencies (Chen <i>et al.</i> , 1993).	13
Figure 2.2: Advantages of microwave processing.	15
Figure 2.3: Fractured section of KFRP (Mahjoub, Yatim, <i>et al.</i> , 2014).....	17
Figure 2.4: Fracture morphology of MWCNT/epoxy composite (a) with surfactant and (b) without surfactant (Gong <i>et al.</i> , 2000).....	20
Figure 2.5: (a) Schematic of multi-directional lay-up composite and (b) LS-DYNA model of the corrugated composite specimen (Duan <i>et al.</i> , 2014).....	23
Figure 2.6: Plan of work.	29
Figure 3.1: Microwave applicator used for the fabrication of composites.	32
Figure 3.2: Images showing (a) HDPE/MWCNT pellets with SEM micrograph, and (b) HDPE pellets.	33
Figure 3.3: SEM micrograph of the treated kenaf fibre mat.....	34
Figure 3.4: Schematic of the experimental setup for HDPE/kenaf polymer composite.	37
Figure 3.5: MACM polymer composite of HDPE/kenaf (a) top view (b) cross-section.....	37
Figure 3.6: Schematic of the experimental setup for HDPE/MWCNT polymer composite. ..	40

Figure 3.7: MACMed HDPE/MWCNT polymer composite.....	40
Figure 3.8: Specimen dimension details for the three-point bend test.....	44
Figure 3.9: Tensile test (a) Engineering stress vs. strain, (b) Load vs. displacement curve....	45
Figure 3.10: SEM fractographs of tensile fractured (a) HDPE/kenaf, (b) HDPE/MWCNT polymer composite.....	47
Figure 3.11: Engineering stress vs. strain curve at different strain rate for (a) HDPE/kenaf, (b) HDPE/MWCNT composite.....	48
Figure 3.12: Stress relaxation curve for (a) HDPE/kenaf, (b) HDPE/MWCNT polymer composite.....	50
Figure 3.13: Flexural tested specimen of (a) HDPE/MWCNT, (b) HDPE/kenaf composite. .	52
Figure 3.14: Flexural (a) Engineering stress vs. strain, (b) Load vs. displacement curve of HDPE/MWCNT and HDPE/kenaf polymer composite.....	52
Figure 3.15: Impact energy vs. angular displacement curves of HDPE/kenaf and HDPE/MWCNT polymer composites.	54
Figure 3.16: SEM fractographs of impact fractured (a) HDPE/kenaf, (b) HDPE/MWCNT polymer composite.....	55
Figure 4.1: Simulation algorithm.....	61
Figure 4.2: Comparison of results for different number of elements w.r.t. Gálvez et al. (2009).....	64
Figure 4.3: (a) Body panel structure, (b) meshed model used for the crashworthiness analysis.	66
Figure 4.4: (a) Full, (b) offset frontal impact side view and (c) oblique frontal impact top view.....	67
Figure 4.5: Directional deformation for full frontal impact on (a,b) structural steel and (c,d) concrete rigid wall.....	71

Figure 4.6: (a) Probe, deformed shape of the bumper for (b) HDPE/kenaf, (c) HDPE/MWCNT and (d) Aluminum alloy (Al5022).	72
Figure 4.7: Reaction force for full frontal impact on (a,b) structural steel and (c,d) concrete rigid wall.	74
Figure 4.8: Kinetic energy for full frontal impact on (a,b) structural steel and (c,d) concrete rigid wall.	75
Figure 4.9: Deformed probe after impact on a rigid wall.	77
Figure 4.10: Directional deformation for offset frontal impact on (a,b) structural steel and (c,d) concrete rigid wall.	78
Figure 4.11: Reaction force for offset frontal impact on (a,b) structural steel and (c,d) concrete rigid wall.....	80
Figure 4.12: Kinetic energy for offset frontal impact on (a,b) structural steel and (c,d) concrete rigid wall.....	81
Figure 4.13: Directional deformation for HDPE/kenaf w.r.t. aluminum alloy (Al5022) upon impact on structural steel rigid wall at (a) 10°, (b) 20° and (c) 30° impact angle.	83
Figure 4.14: Directional deformation for HDPE/MWCNT w.r.t. aluminum alloy (Al5022) upon impact on structural steel rigid wall at (a) 10°, (b) 20° and (c) 30° impact angle.	84
Figure 4.15: Directional deformation for HDPE/kenaf w.r.t. aluminum alloy (Al5022) upon impact on the concrete rigid wall at (a) 10°, (b) 20° and (c) 30° impact angle.	85
Figure 4.16: Directional deformation for HDPE/MWCNT w.r.t. aluminum alloy (Al5022) upon impact on the concrete rigid wall at (a) 10°, (b) 20° and (c) 30° impact angle.	86
Figure 4.17: Reaction force for HDPE/kenaf w.r.t. aluminum alloy (Al5022) upon impact on structural steel rigid wall at (a) 10°, (b) 20° and (c) 30° impact angle.	88
Figure 4.18: Reaction force for HDPE/MWCNT w.r.t. aluminum alloy (Al5022) upon impact on structural steel rigid wall at (a) 10°, (b) 20° and (c) 30° impact angle.	89

Figure 4.19: Reaction force for HDPE/kenaf w.r.t. aluminum alloy (Al5022) upon impact on the concrete rigid wall at (a) 10°, (b) 20° and (c) 30° impact angle.	90
Figure 4.20: Reaction force for HDPE/MWCNT w.r.t. aluminum alloy (Al5022) upon impact on the concrete rigid wall at (a) 10°, (b) 20° and (c) 30° impact angle.	91
Figure 4.21: Change in kinetic energy for HDPE/kenaf w.r.t. aluminum alloy (Al5022) upon impact on structural steel rigid wall at (a) 10°, (b) 20° and (c) 30° impact angle.	93
Figure 4.22: Change in kinetic energy for HDPE/MWCNT w.r.t. aluminum alloy (Al5022) upon impact on structural steel rigid wall at (a) 10°, (b) 20° and (c) 30° impact angle.	94
Figure 4.23: Change in kinetic energy for HDPE/kenaf w.r.t. aluminum alloy (Al5022) upon impact on the concrete rigid wall at (a) 10°, (b) 20° and (c) 30° impact angle.	95
Figure 4.24: Change in kinetic energy for HDPE/MWCNT w.r.t. aluminum alloy (Al5022) upon impact on the concrete rigid wall at (a) 10°, (b) 20° and (c) 30° impact angle.	96
Figure 4.25: Meshed model (a) side view, impact at (b) centre and (c) left side of the bumper.	97
Figure 4.26: von Mises stress at the centre and left side of (a,b) HDPE/kenaf and (c,d) HDPE/MWCNT w.r.t. aluminum alloy when impact occurs on a structural steel pole.	98
Figure 4.27: von Mises stress at the centre and left side of (a,b) HDPE/kenaf and (c,d) HDPE/MWCNT w.r.t. aluminum alloy when impact occurs on the concrete pole.	100
Figure 4.28: Directional deformation at the centre and left side of (a,b) HDPE/kenaf and (c,d) HDPE/MWCNT w.r.t. aluminum alloy when impact occurs on a structural steel pole.	101
Figure 4.29: Directional deformation at the centre and left side of (a,b) HDPE/kenaf and (c,d) HDPE/MWCNT w.r.t. aluminum alloy when impact occurs on a concrete pole.	102
Figure 4.30: Directional deformation contour of aluminum alloy when impacted at centre (a) side view and (b) top view.....	104

Figure 4.31: Directional deformation contour of aluminum alloy when impacted at left side	
(a) side view and (b) top view.....	105
Figure 4.32: Directional deformation contour of HDPE/kenaf when impacted at centre	
(a) side view and (b) top view.....	106
Figure 4.33: Directional deformation contour of HDPE/kenaf when impacted at left side (a)	
side view and (b) top view.....	107
Figure 4.34: Directional deformation contour of HDPE/MWCNT when impacted at centre	
(a) side view and (b) top view.....	108
Figure 4.35: Directional deformation contour of HDPE/MWCNT when impacted at left side	
(a) side view and (b) top view.....	109

List of Tables

Table 2.1: Summary of fibre treatment of natural fibres.	18
Table 2.2: Summary of microwave material processing and NFRC.	24
Table 3.1: Dielectric constant and penetration depth of materials used.	34
Table 3.2: Parametric optimization of HDPE/kenaf polymer composite.	38
Table 3.3: Parametric optimization of HDPE/MWCNT polymer composite.	40
Table 3.4: Optimum process parameters for the MACM of the polymer composites.....	41
Table 3.5: Elastic modulus at different strain rates.....	49
Table 3.6: Flexural properties of HDPE/kenaf and HDPE/MWCNT polymer composites.	53
Table 4.1: Material properties used by Gopalkrishna et al. (2014).	62
Table 4. 2: Validation of numerical results.....	63
Table 4.3: Convergence study of number of elements w.r.t. residual velocity.....	64
Table 4.4: Material properties.....	70
Table 4.5: Directional deformation values for full frontal impact.....	73
Table 4.6: Change in kinetic energy and deceleration for full frontal impact.	76
Table 4.7: Directional deformation values for offset frontal impact.	79
Table 4.8: Change in kinetic energy and deceleration for offset frontal impact.....	82
Table 4.9: Directional deformation values for oblique frontal impact.	87
Table 4.10: Change in kinetic energy and deceleration for oblique frontal impact.....	92

Abstract

The present work deals with a novel manufacturing route, microwave-assisted compression moulding (MACM), for fabricating high-density polyethylene (HDPE) based composites. In the present work, 20 wt.% of reinforcement in the form of kenaf and multi-walled carbon nanotube (MWCNT) was used to fabricate HDPE/kenaf and HDPE/MWCNT polymer composites. The mechanical characterizations of the microwave processed composites were carried out in terms of the uniaxial tensile test at different strain rates, multi-step stress relaxation, flexural and impact test. The uniaxial tensile test revealed that the tensile modulus of four-layered HDPE/kenaf polymer composite was 35.2% higher than that of HDPE/MWCNT polymer composite. The HDPE/MWCNT polymer composite showed elastic modulus a minimum of 1.25 GPa and a maximum of 4.7 GPa when tested at different strain rates. The energy absorbed by the HDPE/kenaf polymer composite (1.055 J) was 81.12% higher than the HDPE/MWCNT polymer composite (0.582 J).

Thereafter, the experimentally obtained properties have been utilized in crashworthiness testing of HDPE composites with respect to the aluminum alloy (Al5022) due to their comparable specific energy absorption. Finite element method (FEM) based ANSYS 16.0 package has been utilized to predict comparative crashworthiness strength of composites. Numerical results were obtained for full, offset and oblique frontal impact of the automobile body panel. Crashworthiness of the automotive body panel has been investigated on the basis of the deformation of the bumper, kinetic energy of the body panel and the reaction force of the target body. Although the directional deformation of the HDPE/kenaf and HDPE/MWCNT composites is higher than the aluminum alloy (Al5022), they have a considerably lower value of deceleration and reaction force during the impact period.

Nomenclature

ACRONYMS

ASTM	American Society for Testing and Materials
DSC	Differential scanning calorimetry
HDPE/MWCNT	High-density polyethylene/multiwalled carbon nanotube-polymer
HDPE/kenaf	High-density polyethylene/kenaf fibre reinforced polymer
MACM	Microwave-assisted compression moulding
NFRC	Natural fibre reinforced composite
NaOH	Sodium hydroxide
SEA	Specific energy absorption
PP	Polypropylene
PE	Polyethylene

SYMBOLS

Vector quantities

B	Body force
Γ	Boundary
σ	Cauchy stress tensor
\ddot{U}_i	Component of nodal acceleration ($i=1,2,3$)
\dot{U}_i	Velocity at nodal point ($i=1,2,3$)
U_i	Componenet of nodal displacement ($i=1,2,3$)
F_i	Component of nodal force ($i=1,2,3$)

S	Stiffness matrix
Scalar quantities	
E	Young's modulus of the polymer composite
e	Volume expansion of the material
E_f	Flexural modulus of the polymer composite
G	The shear modulus of the polymer composite
K	The bulk modulus of the polymer composite
Δk	Change in kinetic energy of body panel
L	Span length of the specimen
m	Mass of the body panel
m_n	Nodal mass
N	Shape function
P	Maximum applied load
s	The slope of the secant of the load-displacement curve
T_g	Glass transition temperature
T	The thickness of the specimen
t	Duration of impact
W	Width of the specimen
ρ	The density of polymer composite
ρ_p	Density of polymer
ρ_r	Density of reinforcement
V_p	The volume fraction of polymer
V_r	The volume fraction of reinforcement

U_0	The initial velocity of the body panel
U_t	The final velocity of the body panel at time 't'
δ	Deflection of the specimen in the flexural test
a	Deceleration of body panel
Ω	Domain
σ_f	Flexural stress of the polymer composite
ε_f	Flexural strain of the polymer composite